Layer-by-Layer Assembled Polyampholyte Microgel Films for Simultaneous Release of Anionic and Cationic Molecules

ARTICLE *in* LANGMUIR · FEBRUARY 2010

Impact Factor: 4.46 · DOI: 10.1021/la904558h · Source: PubMed

5 AUTHORS, INCLUDING:

Xu Wang
State University of New York Upstate Medica…

11 PUBLICATIONS **247** CITATIONS

SEE PROFILE

Langmuir
Article
pubs.acs.org/Langmuir

Layer-by-Layer Assembled Polyampholyte Microgel Films for Simultaneous Release of Anionic and Cationic Molecules

Xu Wang,[†] Lianbin Zhang,[†] Lin Wang,[‡] Junqi Sun,*[,†] and Jiacong Shen[†]

[†]*State Key Laboratory of Supramolecular Structure and Materials, College of Chemistry, Jilin University, Changchun, P. R. China 130012, and* [‡]*College of Science, Northwest Agriculture & Forestry University, Yangling, P. R. China 712100*

Received December 3, 2009. Revised Manuscript Received January 25, 2010

A facile layer-by-layer (LbL) assembly method for the fabrication of matrix films capable of coloading and simultaneous release of oppositely charged molecules has been established by using polyampholyte microgels as building blocks. Polyampholyte microgels (named PAH-D-CO_2) containing amine and carbamate groups were LbL assembled with polyanion poly(sodium 4-styrenesulfonate) (PSS) to produce PAH-D-CO_2/PSS multilayer films. The successful fabrication of PAH-D-CO_2/PSS multilayer films was verified by quartz crystal microbalance measurements and cross-sectional scanning electron microscopy. Anionic methyl orange and cationic rhodamine 6G were coloaded into PAH-D-CO_2/PSS multilayer films because of the electrostatic interaction of these dyes with amine and carbamate groups in the PAH-D-CO_2/PSS microgel films. The abundance of amine and carbamate groups as well as the swelling capacity of PAH-D-CO_2 microgels guarantees the high loading capacity of the PAH-D-CO_2/PSS multilayer films toward the anionic and cationic dyes. Methyl orange and rhodamine 6G were simultaneously released from PAH-D-CO_2/PSS multilayer films when immersing the dye-loaded films into 0.9% normal saline. The releasing behaviors of the polyampholyte microgel films can be tailored by capping the PAH-D-CO_2/PSS films with barrier layers. The polyampholyte microgel films of PAH-D-CO_2/PSS are expected to be widely useful as matrixes for coloading oppositely charged functional guest materials such as drugs and even for their controlled release.

Introduction

The layer-by-layer (LbL) assembly technique has been proven to be a versatile and convenient way to construct composite films with precise control of film thickness and structures.[1] In the past decade, LbL assembled multilayer films as matrixes for controlled release, especially for ionic drug delivery, have received particular attention.[2−4] Compared with other film preparative techniques, the LbL assembly technique has two prominent merits in preparing delivery coatings. First, the loading capacity of the LbL assembled films and the release kinetics of the loaded guest materials can be conveniently and precisely controlled by tailoring the assembly parameters including number of deposition cycles,[5] concentration, ionic strength, and pH of dipping solution[1c] or through post-treatments.[6] Second, the LbL assembly technique is particularly suitable for large area film deposition on irregular surfaces.[7] Postdiffusion[2,8−11] is a frequently employed method to incorporate guest materials into LbL assembled multilayer films because not all of the guest materials can be alternately assembled with a partner species to produce multilayer films. The loading of guest materials by a postdiffusion method depends on the overplus of charged groups in the LbL assembled films, which bind the charged guest materials by electrostatic interaction among them. Previously reported LbL assembled films were used to load only the samely charged guest materials through a postdiffusion process.[2,8−10] Unfortunately, the coloading and simultaneous release of anionic and cationic materials within LbL assembled polymeric films have not been investigated.

Polyampholyte microgels contain both positively and negatively charged groups and provide binding sites for both anionic and cationic species.[12] In the past decade, various polyampholyte microgels have been synthesized.[13] Their swelling[12−14] and electrophoretic[12,13,15] behaviors have been widely investigated. Up to

*To whom correspondence should be addressed: Fax 0086-431-5193421; e-mail sun_junqi@jlu.edu.cn.

(1) (a) Decher, G. *Science* **1997**, *277*, 1232. (b) Hammond, P. T. *Adv. Mater.* **2004**, *16*, 1271. (c) Tang, Z. Y.; Wang, Y.; Podsiadlo, P.; Kotov, N. A. *Adv. Mater.* **2006**, *18*, 3203. (d) Lynn, D. M. *Soft Matter* **2006**, *2*, 269. (e) Quinn, J. F.; Johnston, A. P. R.; Such, G. K.; Zelikin, A. N.; Caruso, F. *Chem. Soc. Rev.* **2007**, *36*, 707. (f) Zhang, X.; Chen, H.; Zhang, H. Y. *Chem. Commun.* **2007**, 1395.

(2) (a) Chung, A. J.; Rubner, M. F. *Langmuir* **2002**, *18*, 1176. (b) Hiller, J.; Rubner, M. F. *Macromolecules* **2003**, *36*, 4078.

(3) Wood, K. C.; Chuang, H. F.; Batten, R. D.; Lynn, D. M.; Hammond, P. T. *Proc. Natl. Acad. Sci. U.S.A.* **2006**, *103*, 10207.

(4) Kharlampieva, E.; Kozlovskaya, V.; Sukhishvili, S. A. *Adv. Mater.* **2009**, *21*, 3053.

(5) Berg, M. C.; Zhai, L.; Cohen, R. E.; Rubner, M. F. *Biomacromolecules* **2006**, *7*, 357.

(6) Zhang, H. Y.; Fu, Y.; Wang, D.; Wang, L. Y.; Wang, Z. Q.; Zhang, X. *Langmuir* **2003**, *19*, 8497.

(7) (a) Caruso, F.; Caruso, R. A.; Möhwald, H. *Science* **1998**, *282*, 1111. (b) Ai, S. F.; Lu, G.; He, Q.; Li, J. B. *J. Am. Chem. Soc.* **2003**, *125*, 11140. (c) Jewell, C. M.; Zhang, J.; Fredin, N. J.; Wolff, M. R.; Hacker, T. A.; Lynn, D. M. *Biomacromolecules* **2006**, *7*, 2483. (d) Podsiadlo, P.; Arruda, E. M.; Kheng, E.; Waas, A. M.; Lee, J.; Critchley, K.; Qin, M.; Chuang, E.; Kaushik, A. K.; Kim, H.-S.; Qi, Y.; Noh, S.-T.; Kotov, N. A. *ACS Nano* **2009**, *3*, 1564.

(8) Wang, L.; Wang, X.; Xu, M. F.; Chen, D. D.; Sun, J. Q. *Langmuir* **2008**, *24*, 1902.

(9) Wang, L.; Chen, D. D.; Sun, J. Q. *Langmuir* **2009**, *25*, 7990.

(10) (a) Quinn, J. F.; Caruso, F. *Langmuir* **2004**, *20*, 20. (b) Guyomard, A.; Nysten, B.; Muller, G.; Glinel, K. *Langmuir* **2006**, *22*, 2281.

(11) Burke, S. E.; Barrett, C. J. *Macromolecules* **2004**, *37*, 5375.

(12) (a) Neyret, S.; Vincent, B. *Polymer* **1997**, *38*, 6129. (b) Das, M.; Kumacheva, E. *Colloid Polym. Sci.* **2006**, *284*, 1073.

(13) (a) Ogawa, K.; Nakayama, A.; Kokufuta, E. *Langmuir* **2003**, *19*, 3178. (b) Tan, B. H.; Ravi, P.; Tam, K. C. *Macromol. Rapid Commun.* **2006**, *27*, 522. (c) Bradley, M.; Vincent, B.; Burnett, G. *Aust. J. Chem.* **2007**, *60*, 646. (d) Tan, B. H.; Ravi, P.; Tan, L. N.; Tam, K. C. *J. Colloid Interface Sci.* **2007**, *309*, 453. (e) Ho, B. S.; Tan, B. H.; Tan, J. P. K.; Tam, K. C. *Langmuir* **2008**, *24*, 7698. (f) Das, M.; Sanson, N.; Kumacheva, E. *Chem. Mater.* **2008**, *20*, 7157. (g) Bradley, M.; Liu, D.; Keddie, J. L.; Vincent, B.; Burnett, G. *Langmuir* **2009**, *25*, 9677.

(14) (a) Nisato, G.; Munch, J. P.; Candau, S. J. *Langmuir* **1999**, *15*, 4236. (b) Hampton, K. W.; Ford, W. T. *Macromolecules* **2000**, *33*, 7292. (c) Sutani, K.; Kaetsu, I.; Uchida, K.; Matsubara, Y. *Radiat. Phys. Chem.* **2002**, *64*, 331.

(15) Ogawa, K.; Nakayama, A.; Kokufuta, E. *J. Phys. Chem. B* **2003**, *107*, 8223.

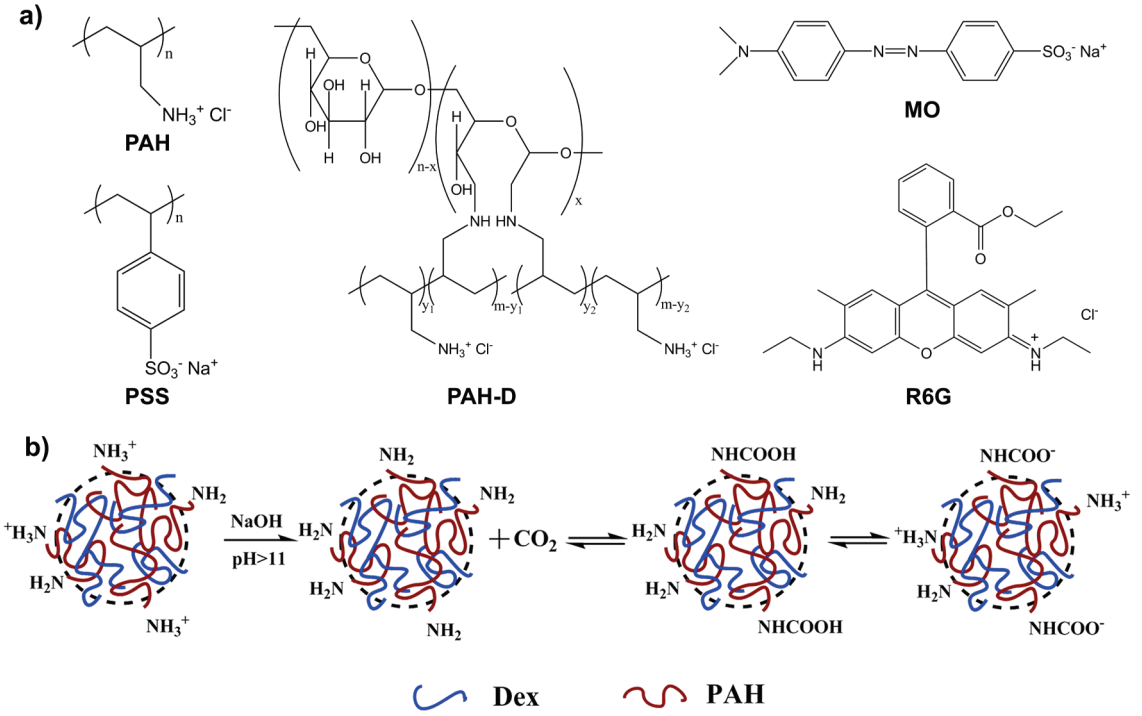

Figure 1. (a) Chemical structures of PAH, PSS, MO, R6G, and PAH-D. (b) Schematic illustration of the synthesis of PAH-D-CO_2 microgels. There are amine and carbamate groups at both the exterior and the interior of PAH-D-CO_2 microgels. For simplicity, the interior groups are not shown in the illustration.

now, polyampholyte microgels have found useful applications in the delivery of guest materials in solution[13g,14c] and template-based synthesis of inorganic nanoparticles.[13f] However, as far as we know, there is no report concerning the fabrication of LbL assembled films by using polyampholyte microgels as building blocks, not to mention the application of such films in controlled delivery.

Recently, a type of LbL assembled polymeric microgel films with high loading capacity was prepared in our previous work.[8,9] The primary building blocks of the polymeric microgel films were a kind of polymeric microgels synthesized by cross-linking PAH and dextran (noted as PAH-D). The LbL assembled polymeric microgel films of PAH-D/polyanion can incorporate negatively charged small molecules and CdTe nanoparticles with high loading capacity due to a large amount of amine groups in LbL assembled polymeric microgel films.[8,9] In this paper, we demonstrate that LbL assembled polyampholyte microgel films are successful in coloading and simultaneous release of oppositely charged methyl orange (MO) and rhodamine 6G (R6G). The cation-rich polyampholyte microgels containing amine and carbamate groups (named PAH-D-CO_2) were easily prepared by bubbling CO_2 into aqueous solution of PAH-D microgels. The LbL assembled multilayer films comprising alternately deposited PAH-D-CO_2 microgel and poly(sodium 4-styrenesulfonate) (PSS) can incorporate an abundant amount of anionic and cationic molecules and realize their simultaneous release in 0.9% normal saline. Capping the PAH-D-CO_2/PSS films with photo-cross-linkable barrier layers can slow down the release kinetics of dyes from the polyampholyte microgel films. The present study has established a facile LbL assembly method to incorporate oppositely charged species into matrix films of polyampholyte microgels for their simultaneous as well as sustainable release.

Experimental Section

Materials. Poly(allylamine hydrochloride) (PAH, M_w ca. 52 000), poly(sodium 4-styrenesulfonate) (PSS, M_w ca. 70 000), and rhodamine 6G (R6G) were purchased from Sigma-Aldrich. Methyl orange (MO) was purchased from Beijing Chemical Reagents Co. The chemical structures of PAH, PSS, MO, and R6G are shown in Figure 1a. Dextran (M_w ca. 40 000) was purchased from Tokyo Chemical Industry Co., Ltd. Here PAH and dextran were used for the synthesis of PAH-D microgels. Diazoresin (DAR, the structure is shown in the inset of Figure 5b) was synthesized according to a literature procedure.[16] The molecular weight (M_n) of the DAR was ~2640. All other chemicals were of analytical reagent grade and used as received. Deionized water was used for all the experiments.

Synthesis of Polyampholyte PAH-D-CO_2 Microgels. PAH-D microgels containing amine groups were synthesized by cross-linking PAH and dextran, as reported in our previous publication.[8,17,18] The PAH-D microgels contain PAH and dextran with a monomer molar ratio of 1.5:1. To synthesize polyampholyte PAH-D-CO_2 microgels, CO_2 gas was bubbled through a 30 mL aqueous solution containing 30 mg PAH-D microgels for ~15 min to reach a final solution pH of ~6.5. Parts of amine groups in PAH-D microgels were converted into carbamate groups,[19] and polyampholyte PAH-D-CO_2 microgels containing amine and carbamate groups were obtained.

Film Preparation. Ag-coated quartz crystal microbalance (QCM) resonators were sonicated slightly in ethanol and water and were dried by N_2 flow. Quartz and silicon wafers were immersed in piranha solution (1:3 mixture of 30% H_2O_2 and 98% H_2SO_4) and heated until no bubbles were released. These cleaned substrates are suitable for LbL deposition of PAH-D-CO_2/PSS multilayer films without further substrate modification.

(16) Cao, W. X.; Ye, S. J.; Cao, G. S.; Zhao, C. *Macromol. Rapid Commun.* **1997**, *18*, 983.
(17) Wang, L.; Sun, J. Q. *J. Mater. Chem.* **2008**, *18*, 4042.
(18) Wang, X.; Zhou, S. Y.; Lai, Y.; Sun, J. Q.; Shen, J. C. *J. Mater. Chem.* **2010**, *20*, 555.
(19) (a) George, M.; Weiss, R. G. *J. Am. Chem. Soc.* **2001**, *123*, 10393. (b) George, M.; Weiss, R. G. *Langmuir* **2002**, *18*, 7124. (c) Rudkevich, D. M.; Xu, H. *Chem. Commun.* **2005**, 2651. (d) Alauzun, J.; Mehdi, A.; Reyé, C.; Corriu, R. J. P. *J. Am. Chem. Soc.* **2005**, *127*, 11204. (e) Alauzun, J.; Besson, E.; Mehdi, A.; Reyé, C.; Corriu, R. J. P. *Chem. Mater.* **2008**, *20*, 503.

The deposition of PAH-D-CO_2/PSS multilayer films is commenced with the PAH-D-CO_2 layer because PAH-D-CO_2 can be deposited directly on the surface of silver and quartz substrates. The substrate was first immersed in a PAH-D-CO_2 aqueous solution (1.0 mg/mL) for 20 min, washed with ample water, and blown dry with N_2 flow. The substrate was then transferred to an aqueous PSS solution (1.0 mg/mL) for 20 min, washed with ample water, and blown dry with N_2 flow. By repetition of the above deposition processes in a cyclic fashion, multilayer film of PAH-D-CO_2/PSS can be fabricated. All films were prepared at a solution pH of 7.4. The pH of PAH-D-CO_2 and PSS solutions was adjusted with either 1 M HCl or 1 M NaOH.

Barrier Layer Deposition. The LbL deposition of DAR/PSS barrier layers on top of the PAH-D-CO_2/PSS films was conducted in the dark.[20] The substrate deposited with PAH-D-CO_2/PSS multilayer films was alternately immersed in an aqueous solution of DAR (1.0 mg/mL, pH 3.0) and PSS (1.0 mg/mL, pH 3.0) for 20 min, with intermediate water rinsing and N_2 drying. Multilayer films of DAR/PSS can be fabricated by repeating these steps in a cyclic fashion. Photo-cross-linking of the DAR/PSS multilayer films was conducted by irradiating the films with a 40 W UV lamp at a distance of 10 cm from the source for 30 min.

Loading and Release of Dyes. Independent loading of MO and R6G molecules into the LbL assembled PAH-D-CO_2/PSS multilayer films was realized by immersing the films into aqueous solution of MO (15.0 mM, pH 7.4) and R6G (15.0 mM, pH 7.4), respectively. The coloading of oppositely charged MO and R6G molecules was accomplished as follows: First, saturation loading of MO was accomplished by immersing the LbL assembled PAH-D-CO_2/PSS multilayer films into aqueous solution of MO (15.0 mM, pH 7.4). Then the films were immersed into aqueous solution of R6G (15.0 mM, pH 7.4). A reverse sequence can also work for coloading of MO and R6G molecules. To study the loading kinetics, the films deposited on quartz slides were taken out from MO or R6G solution for a given time, rinsed with an ample amount of water, and dried with N_2 flow for UV−vis absorption spectroscopy measurements. To investigate the release kinetics, the dye-loaded films deposited on quartz slides were immersed into a beaker containing 3.5 mL of 0.9% normal saline. The 0.9% normal saline was frequently replaced by a fresh one to ensure constant release conditions. The amounts of MO and R6G released from the films were determined using a calibration curve for MO and R6G in 0.9% normal saline because the absorbance of released MO and R6G in 0.9% normal saline obeyed Beer's law.

Characterization. Fourier transform infrared (FTIR) spectra were recorded on a Bruker VERTEX-80 V instrument. Dynamic light scattering (DLS) studies and electrophoretic measurements of polymeric microgels were carried out on a Malvern Nano-ZS zetasizer at room temperature. The measurements were made at a scattering angle of $\theta = 173°$ at 25 °C using a He−Ne laser with a wavelength of 633 nm. QCM measurements were taken with a KSV QCM-Z500 using quartz resonators with both sides coated with Ag (F_0 = 9 MHz). Scanning electron microscopy (SEM) images were obtained on an XL30 ESEM FEG scanning electron microscope. The PAH-D-CO_2/PSS films deposited on silicon wafers were cleaved, and their cross-sectional SEM images were recorded. All samples were coated with a thin layer of gold (2−3 nm) prior to SEM imaging. UV−vis absorption spectra were recorded on a Shimadzu UV-2550 spectrophotometer.

Results and Discussion

Synthesis and Characterization of PAH-D-CO_2 Microgels. As shown in Figure 1a, PAH-D microgels are cross-linked PAH and dextran, which contain abundance of free amine groups.[8,17,18]

(20) (a) Sun, J. Q.; Wu, T.; Sun, Y. P.; Wang, Z. Q.; Zhang, X.; Shen, J. C.; Cao, W. X. *Chem. Commun.* **1998**, 1853. (b) Sun, J. Q.; Wang, Z. Q.; Wu, L. X.; Zhang, X.; Shen, J. C.; Gao, S.; Chi, L. F.; Fuchs, H. *Macromol. Chem. Phys.* **2001**, *202*, 967.

Table 1. Electrophoretic Mobility and *z*-Average Diameter of PAH-D-CO_2 and PAH-D Microgels at a Solution pH of 7.4 with and without the Addition of NaCl[a]

microgels at pH 7.4	mobility (μm cm/(V s))[b]	diameter (nm)[b]
PAH-D-CO_2 without NaCl	1.9 ± 0.2	255 ± 6
PAH-D-CO_2 with 0.2 M NaCl	1.1 ± 0.1	227 ± 12
PAH-D without NaCl	3.7 ± 0.1	460 ± 39
PAH-D with 0.2 M NaCl	1.3 ± 0.1	222 ± 5

[a] Measurements were made in aqueous solution with a polymeric microgel concentration of 1 mg/mL. [b] The error is for standard deviation (n = 3).

Figure 1b is the schematic illustration of the synthesis of PAH-D-CO_2 microgels. The synthesis of polyampholyte PAH-D-CO_2 microgels was conducted by bubbling CO_2 into aqueous PAH-D solution with an initial pH of 11.0 because the reaction of amine groups and CO_2 usually takes place in polar aprotic solvents.[21] After CO_2 gas was bubbled through the aqueous PAH-D solution, a part of amine groups of PAH-D microgels were converted into carbamate groups with a decrease of solution pH. The presence of amine and carbamate groups in PAH-D-CO_2 microgels was confirmed by the FTIR spectra of PAH-D and PAH-D-CO_2 microgels casted on silicon wafers. The band at 1626 cm^{-1} is assigned to the scissoring bending of −N−H of amine groups in FTIR spectrum of PAH-D microgels.[8] The FTIR spectrum of PAH-D-CO_2 microgels shows a new band at about 1573 cm^{-1}, which is assigned to the $NHCOO^-$ group of the carbamate anion.[22] Meanwhile, the band at 1626 cm^{-1} still exists in the FTIR spectrum of PAH-D-CO_2 microgels, indicating that only a partial amine groups in PAH-D-CO_2 microgels are converted into carbamate groups. FTIR spectroscopy provides a semiquantitative way to determine the conversion degree of amine groups to carbamate groups. During the reaction, the FTIR intensity of ether groups and methylene groups in PAH-D-CO_2 microgels do not change and can be used as references to calculate the conversion degree. About 37% of the amine groups in PAH-D microges are converted to carbamate groups in PAH-D-CO_2 microgels when taking the FTIR intensities of C−O stretching vibrations at 1019, 1039, and 1152 cm^{-1} and C−H stretching vibration at 2919 cm^{-1} as references.

The electrophoretic mobilities and *z*-average diameters of PAH-D and PAH-D-CO_2 microgels in water with and without the addition of 0.2 M NaCl at an invariable pH of 7.4 were investigated and shown in Table 1. Without the addition of NaCl, PAH-D microgels in water have a *z*-average diameter of 460 ± 39 nm and electrophoretic mobility of 3.7 ± 0.1 μm cm/(V s), while PAH-D-CO_2 microgels have a smaller *z*-average diameter of 255 ± 6 nm and lower electrophoretic mobility of 1.9 ± 0.2 μm cm/(V s). Parts of amine groups in PAH-D microgels are converted into carbamate groups in the resultant PAH-D-CO_2 microgels. Therefore, the intensity of charge−charge repulsion in the network of PAH-D-CO_2 microgels is weaker than that in PAH-D microgels. The reduced charge−charge repulsion leads to a decrease of *z*-average diameter and electrophoretic mobility in PAH-D-CO_2 microgels compared with PAH-D microgels. The high concentration of inorganic ions in PAH-D and PAH-D-CO_2 microgel solution with 0.2 M NaCl can screen the charged groups in PAH-D and PAH-D-CO_2 microgels. As a result, the

(21) (a) Hampe, E. M.; Rudkevich, D. M. *Chem. Commun.* **2002**, 1450. (b) Dell'Amico, D. B.; Calderazzo, F.; Labella, L.; Marchetti, F.; Pampaloni, G. *Chem. Rev.* **2003**, *103*, 3857.

(22) (a) Khann, R. K.; Moore, M. H. *Spectrochim. Acta, Part A* **1999**, *55*, 961. (b) Masuda, K.; Ito, Y.; Horiguchi, M.; Fujita, H. *Tetrahedron* **2005**, *61*, 213. (c) Ito, Y.; Ushitora, H. *Tetrahedron* **2006**, *62*, 226.

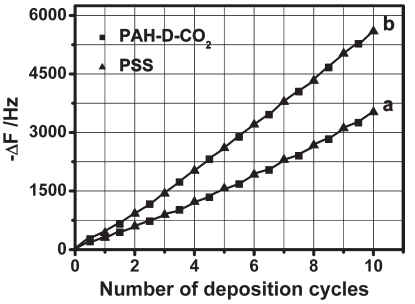

Figure 2. Typical QCM frequency decreases for the alternate deposition of PAH-D-CO_2/PSS multilayer films in water solutions (a) and in 0.2 M aqueous NaCl solution (b). ■ and ▲ represent the frequency decreases upon the deposition of PAH-D-CO_2 and PSS, respectively.

charge−charge repulsion reduces, which leads to a decrease of *z*-average diameter and electrophoretic mobility of PAH-D and PAH-D-CO_2 microgels when compared with those in water without NaCl addition.[14a]

Preparation of PAH-D-CO_2/PSS Multilayer Films. PAH-D-CO_2 microgels are cation-rich in neutral aqueous solution as revealed by their electrophoretic mobility measurements, which can be LbL assembled with polyanion PSS based on electrostatic interaction as the main driving force to prepare PAH-D-CO_2/PSS multilayer films. QCM measurements were employed to monitor the deposition process of PAH-D-CO_2/PSS multilayer films. PAH-D-CO_2 microgels can be deposited directly on QCM resonators because amine and carbonate groups can coordinate with silver surface. Figure 2 shows the decreases of frequency as a function of the layer number for PAH-D-CO_2 and PSS without and with the addition of 0.2 mol/L NaCl in the PAH-D-CO_2 and PSS dipping solutions at a pH of 7.4. In either case, the QCM frequency regularly decreases because of the successive deposition of PAH-D-CO_2/PSS multilayers on the resonators. The frequency decreases for the deposition of one layer of PAH-D-CO_2 and PSS were 134.7 ± 30.5 and 217.4 ± 61.5 Hz, respectively, when dipping solutions of PAH-D-CO_2 and PSS without NaCl addition were used. With the addition of 0.2 mol/L NaCl in the dipping solutions, the frequency decreases for the deposition of one layer of PAH-D-CO_2 and PSS increased to be 270.8 ± 31.5 and 288.5 ± 53.7 Hz, respectively. With the addition of NaCl, PAH-D-CO_2 microgels adopt a more contracted configuration, and their surface charge density decreases. The decrease of surface charge density reduces the repulsion among neighboring PAH-D-CO_2 microgels. The contracted configuration and the reduced repulsion favor a densely adsorbed PAH-D-CO_2 layer on top of the PSS layer.[8] Therefore, the addition of 0.2 mol/L NaCl in the dipping solutions leads to a larger amount of PAH-D-CO_2 deposition. The PAH-D-CO_2 microgels, which are critical for guest material loading, have a higher ratio to PSS in PAH-D-CO_2/PSS films fabricated when dipping solutions with higher ionic strength are used. Therefore, the PAH-D-CO_2/PSS films fabricated by using dipping solutions with the addition of 0.2 mol/L NaCl at a pH of 7.4 were employed as matrix coatings to ensure a high loading amount of anionic and cationic molecules.

Independent Loading and Release of Anionic and Cationic Molecules. Owing to their similar molecular weight and dimensions with daily used drugs and the easy detection by spectroscopic means, organic dyes of negatively charged methyl orange (MO) and positively charged rhodamine 6G (R6G) are employed as model drugs to investigate the loading and release properties of PAH-D-CO_2/PSS films. The independent loading and release process of MO and R6G in (PAH-D-CO_2/PSS)*10 films deposited on quartz slides was monitored by UV−vis absorption spectroscopy. Like PAH-D microgels, the direct deposition of PAH-D-CO_2 microgels on quartz was achieved mainly based on electrostatic interaction and hydrogen bonding between amine groups of PAH-D-CO_2 microgel and silanol groups on a quartz surface.[8] As shown in Figure 3A, the as-prepared (PAH-D-CO_2/PSS)*10 film has an absorption peak at 225 nm, which is attributed to the absorbance of benzene groups in PSS. After immersion of the (PAH-D-CO_2/PSS)*10 film in aqueous MO solution for 20 min, two new absorption peaks at 268 and 433 nm appear (Figure 3A), indicating the successful loading of MO within the (PAHD-CO_2/PSS)*10 films. Electrostatic interaction of MO and PAH-D-CO_2 is the main driving force for the loading of MO within (PAH-D-CO_2/PSS)*10 films. The inset of Figure 3A shows the absorbance of MO-loaded PAH-D-CO_2/PSS films at 433 nm as a function of the number of PAH-D-CO_2/PSS deposition cycles. In each case, saturation loading of MO in PAH-D-CO_2/PSS film was realized. The linear increase of the absorbance at 433 nm with the number of film deposition cycles supports that MO molecules are loaded homogeneously along the normal direction of the whole PAH-D-CO_2/PSS films rather than only on the surfaces. The thickness-dependent dye loading in PAH-D-CO_2/PSS films makes it easy to control the amount of dyes loaded by simply changing the number of film deposition cycles. After immersion of the MO-loaded (PAH-D-CO_2/PSS)*10 films in 0.9% normal saline for 45 min, the absorbance at 268 and 433 nm decreases dramatically, confirming the complete release of MO in 0.9% normal saline. The electrostatic interaction between MO and PAH-D-CO_2 microgel was broken in solution of high ionic strength. Therefore, the release of MO from the PAH-D-CO_2/PSS film was achieved.

Figure 3B,C shows the loading and release profiles of MO molecules when a (PAH-D-CO_2/PSS)*10 film is employed. As shown in Figure 3B, when a 15 mM aqueous MO solution was used, saturation loading of MO molecules in the (PAH-D-CO_2/PSS)*10 film was achieved within 20 min immersion. This result shows that the incorporation of MO into the PAH-D-CO_2/PSS multilayer films proceeds very rapidly. The loading behavior of MO in PAH-D-CO_2/PSS films is similar to that in PAH-D/PSS films.[8] After the loading of MO, the colorless film of PAH-D-CO_2/PSS turns to yellow (inset of Figure 3B). Figure 3C shows the time-dependent release profile of MO molecules from MO-loaded (PAH-D-CO_2/PSS)*10 film in 0.9% normal saline. For the initial 10 min, ~90% of the MO molecules were released from the film. The release process completed within 45 min. The maximum loading amount of MO molecules in PAH-D-CO_2/PSS film is calculated to be ~0.23 $\mu g/cm^2$/bilayer, which corresponds to $\sim 7.0 \times 10^{-7}$ $mmol/cm^2$/bilayer.

After immersion of the (PAH-D-CO_2/PSS)*10 film in aqueous R6G solution, two new absorption peaks at 353 and 544 nm appear (Figure 3D), indicating the successful loading of R6G in the (PAH-D-CO_2/PSS)*10 film. Electrostatic interaction of R6G and the anionic carbamate groups of PAH-D-CO_2 is the main driving force for the loading of R6G within (PAH-D-CO_2/PSS)*10 film. Meanwhile, the uncomplexed sulfonate groups of PSS also have the ability to load R6G molecules.[23] The loaded R6G in PAH-D-CO_2/PSS films can be released in 0.9% normal saline, as the case for release of MO in PAH-D-CO_2/PSS films. A homogeneous distribution of R6G in PAH-D-CO_2/PSS films was also confirmed in the inset of Figure 3D.

(23) Wang, B.; Gao, C. Y.; Liu, L. L. *J. Phys. Chem. B* **2005**, *109*, 4887.

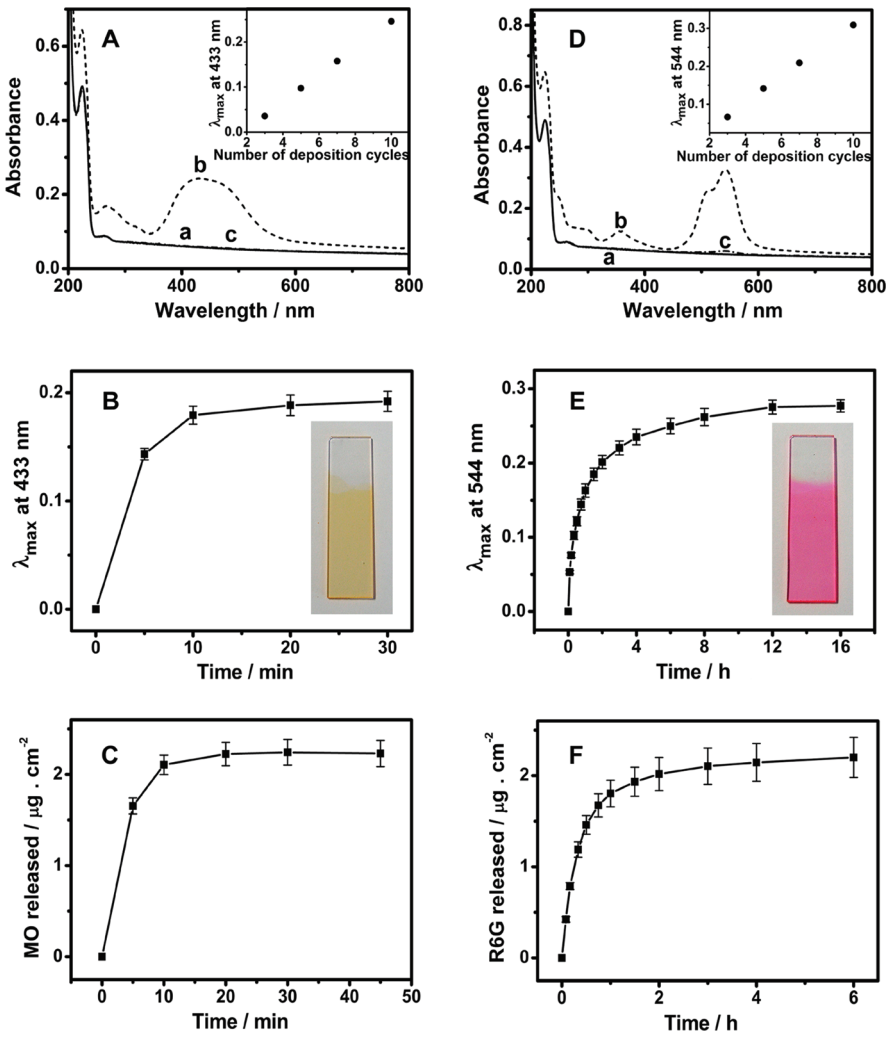

Figure 3. (A) UV−vis absorption spectra of as-prepared (PAH-D-CO_2/PSS)*10 films (a), films in (a) after saturation loading of MO molecules (b), films in (b) after release of MO molecules (c). Inset in (A) is the absorbance of MO-loaded PAH-D-CO_2/PSS films at 433 nm as a function of the number of film deposition cycles. (B, C) Time-dependent loading (B) and release (C) profiles of MO molecules in a (PAH-D-CO_2/PSS)*10 film. Inset in (B) is the photograph of (PAH-D-CO_2/PSS)*10 film after loading of MO molecules. (D) UV−vis absorption spectra of as-prepared (PAH-D-CO_2/PSS)*10 films (a), films in (a) after saturation loading of R6G molecules (b), films in (b) after release of R6G molecules (c). Inset in (D) shows the absorbance of R6G-loaded PAH-D-CO_2/PSS films at 544 nm as a function of the number of film deposition cycles. (E, F) Time-dependent loading (E) and release (F) profiles of R6G molecules in a (PAH-D-CO_2/PSS)*10 film. Inset in (E) is the photograph of (PAH-D-CO_2/PSS)*10 film after loading of R6G molecules. All releases were performed in 0.9% normal saline.

Figure 3E,F shows the loading and release profiles of R6G molecules when a (PAH-D-CO_2/PSS)*10 film is employed. When a 15 mM aqueous R6G solution was used, a saturation loading of R6G molecules in the (PAH-D-CO_2/PSS)*10 film was achieved within 12 h immersion (Figure 3E). The film after loading of R6G shows a pink color of R6G (inset of Figure 3E). In the same loading concentration, the slower loading kinetics of R6G molecules in the (PAH-D-CO_2/PSS)*10 film than MO is possibly due to the larger molecule size and the higher hydrophobicity of R6G which blocks the diffusion of R6G molecules into (PAH-D-CO_2/PSS)*10 film. The larger molecule size and the higher hydrophobicity of R6G also result in more sustainable release of R6G molecules in 0.9% normal saline than MO molecules (Figure 3F). For the initial 1 h, R6G molecules were rapidly released with a release ratio of ~82%. Then the remaining R6G molecules were gradually released. After 6 h in 0.9% normal saline, almost all the R6G molecules were released from the film. The maximum loading amount of R6G molecules in PAH-D-CO_2/PSS films is ~0.22 μg/cm^2/bilayer, which corresponds to ~4.6×10^{-7} mmol/cm^2/bilayer.

We conclude that the carbamate groups in the LbL assembled PAH-D-CO_2/PSS films take the main role in loading of R6G, rather than sulfonate groups in PSS based on the following facts: (i) PAH-D/PSS films which are prepared under the same condition with that of PAH-D-CO_2/PSS film almost cannot load positively charged dyes, as confirmed in our previous study.[8] This result reveals that almost all sulfonate groups of PSS complex with amine groups of PAH-D microgels in PAH-D/PSS films. This might be also the case for PSS in PAH-D-CO_2/PSS films because they are LbL deposited under the same condition with PAH-D/PSS films. (ii) The PAH-D-CO_2 cast films are capable of loading positively charged R6G. After immersing the PAH-D-CO_2 cast film into aqueous solution of positively charged R6G, an absorption peak at 536 nm appears, indicating the successful loading of R6G into the PAH-D-CO_2 cast film. Therefore, we assume that the loading of positively charged R6G molecules is mainly attributed to the carbamate groups in PAH-D-CO_2 microgels although the sulfonate groups in PSS also have the possibility to bind R6G molecules.

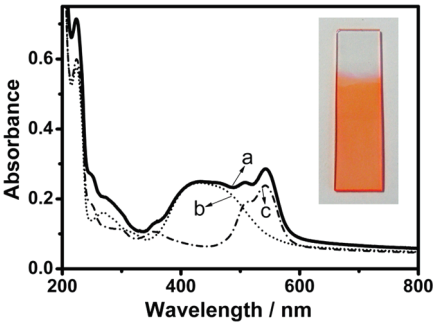

Figure 4. (a) UV−vis absorption spectrum of as-prepared (PAH-D-CO_2/PSS)*10 films after coloading of MO and R6G molecules. (b) and (c) are the peak fittings of (a). Inset is the photograph of (PAH-D-CO_2/PSS)*10 films after coloading of MO and R6G molecules.

Coloading and Simultaneous Release of Anionic and Cationic Molecules. The successful loading of anionic MO and cationic R6G independently in PAH-D-CO_2/PSS films reveals that there is an abundance of positively and negatively charged binding sites in PAH-D-CO_2/PSS films, which can be used for the coloading of oppositely charged guest materials. The coloading of MO and R6G in PAH-D-CO_2/PSS films was then examined. The mixture solution of MO and R6G leads to precipitate because of the strong electrostatic interaction between them. Therefore, the coloading of MO and R6G was performed by first immersing the polyampholyte microgel films into aqueous MO solution and then in R6G solution. The coloading and simultaneous release of MO and R6G in a (PAH-D-CO_2/PSS)*10 film was confirmed by UV−vis absorption spectroscopy. As shown in Figure 4, after immersion of the (PAH-D-CO_2/PSS)*10 film in aqueous MO and R6G solutions, the characteristic absorption peaks of MO at 433 nm and R6G at 544 nm appear, indicating the successful coloading of MO and R6G within the PAH-D-CO_2/PSS multilayer films. The (PAH-D-CO_2/PSS)*10 film after coloading of MO and R6G turns orange (inset in Figure 4), which is different from the color when only one kind of dye is loaded. The absorptions of MO and R6G overlap partially with each other. The amounts of MO and R6G loaded in the PAH-D-CO_2/PSS films are determined by using the simultaneous eq 1:[24]

$$\begin{cases} A_{\lambda_1}^{\mathrm{MO+R6G}} = \varepsilon_{\lambda_1}^{\mathrm{MO}} c^{\mathrm{MO}} + \varepsilon_{\lambda_1}^{\mathrm{R6G}} c^{\mathrm{R6G}} \\ A_{\lambda_2}^{\mathrm{MO+R6G}} = \varepsilon_{\lambda_2}^{\mathrm{MO}} c^{\mathrm{MO}} + \varepsilon_{\lambda_2}^{\mathrm{R6G}} c^{\mathrm{R6G}} \end{cases} \quad (1)$$

Herein, λ_1 and λ_2 are the maximum absorption wavelengths of MO and R6G, $A_{\lambda_1}^{\mathrm{MO+R6G}}$ and $A_{\lambda_2}^{\mathrm{MO+R6G}}$ are the absorbances of MO and R6G in the PAH-D-CO_2/PSS films at λ_1 and λ_2 respectively, and c^{MO} and c^{R6G} are the concentrations of MO and R6G in the (PAH-D-CO_2/PSS)*10 films. The coefficients of $\varepsilon_{\lambda_1}^{\mathrm{MO}}$, $\varepsilon_{\lambda_1}^{\mathrm{R6G}}$, $\varepsilon_{\lambda_2}^{\mathrm{MO}}$, and $\varepsilon_{\lambda_2}^{\mathrm{R6G}}$ can be acquired from the corresponding UV−vis spectrum of each dyes. For (PAH-D-CO_2/PSS)*10 film after coloading of MO and R6G, c^{MO} and c^{R6G} were calculated by eq 1, and then peak fittings of spectrum a in Figure 4 were performed based on c^{MO} and c^{R6G}. In this way, UV−vis absorption spectra of each dyes in the (PAH-D-CO_2/PSS)*10 film were obtained (spectra b and c in Figure 4). It is noteworthy that the absorption of PAH-D-CO_2/PSS film should be deducted before peak fitting analysis to eliminate the background interference. MO and R6G are anion and cation dyes containing one charged group in each molecule. Theoretically, when MO molecules are loaded into PAH-D-CO_2/PSS films by electrostatic interaction between sulfonate groups of MO and amine groups of PAH-D-CO_2 microgels, there is no surplus sulfonate group in MO for binding R6G. When the MO-loaded films are immersed into R6G aqueous solution, a very small amount of MO molecules can be released from the films because the electrostatic interaction between MO and amine groups in PAH-D-CO_2 microgels can be broken by R6G. R6G-MO complexes form which might exist in the PAH-D-CO_2/PSS films. However, R6G-MO complexes are hydrophobic, and their interaction with the PAH-D-CO_2/PSS films is very weak. We assume that if there are R6G-MO complexes formed during the coloading of MO and R6G, they can be easily removed from the PAH-D-CO_2/PSS films by water rinsing. Therefore, the R6G loaded by electrostatic interaction with MO can be negligible.

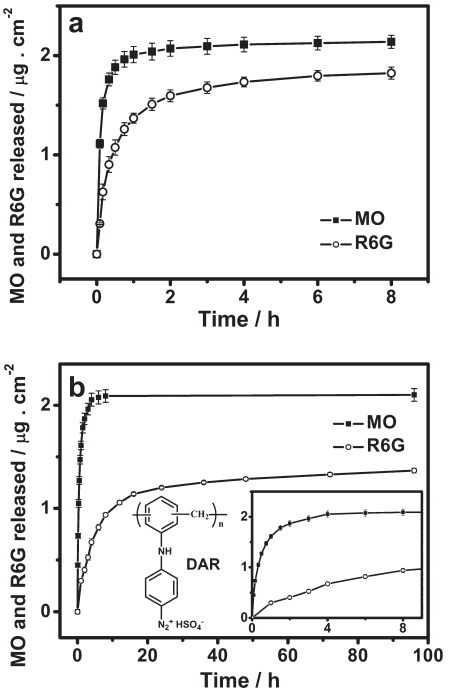

Figure 5. Time-dependent simultaneous release profiles of MO and R6G molecules in a (PAH-D-CO_2/PSS)*10 film (a) and a (PAH-D-CO_2/PSS)*10 film capped with a cross-linked (DAR/PSS)*4 barrier layer (b). Insets in (b) are chemical structure of DAR and the release profile during the first 9 h. The error bars are for standard deviation ($n = 3$).

Figure 5a shows the simultaneous release profile of MO and R6G molecules when a (PAH-D-CO_2/PSS)*10 film is employed. When immersing the (PAH-D-CO_2/PSS)*10 film coloaded with MO and R6G in 0.9% normal saline, MO and R6G molecules released simultaneously. Like the release behavior of the (PAH-D-CO_2/PSS)*10 film loaded with single kind of dyes, the release of MO proceeds fast while R6G slow. The simultaneous release of the MO and R6G from the (PAH-D-CO_2/PSS)*10 film is a bit slower than their independent release from the same (PAH-D-CO_2/PSS)*10 film. Calculated from eq 1, the coloading amounts of MO and R6G molecules in PAH-D-CO_2/PSS film were ~0.22 and ~0.18 μg/cm^2/bilayer, respectively. Actually, the release of MO and R6G from the (PAH-D-CO_2/PSS)*10 film is rapid. We demonstrate that capping the (PAH-D-CO_2/PSS)*10 films with barrier layers of photo-cross-linkable DAR/PSS films can slow down the diffusion of MO and R6G molecules from the polyampholyte microgel films and therefore their release kinetics.

(24) Glenn, A. L. *J. Pharm. Pharmacol.* **1960**, *12*, 595.

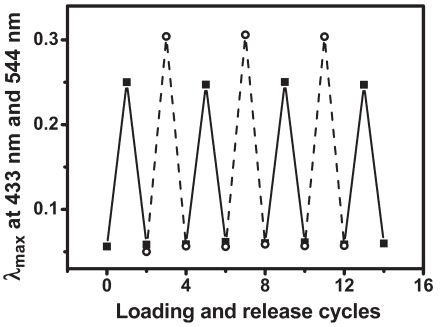

Figure 6. Multiple loading and release behavior of a (PAH-D-CO_2/PSS)*10 film for MO (■) and R6G (○) as monitored by the absorbance at 433 and 544 nm, respectively.

The concept of barrier layers was first proposed by Lynn and Hammond to realize an extended release of drugs from hydrolytically degradable multilayer films.[3] The (PAH-D-CO_2/PSS)*10 films capped with a barrier of (DAR/PSS)*4 films were sequentially loaded with MO and R6G in the dark, as in the case for pure (PAH-D-CO_2/PSS)*10 films. Then the MO- and R6G-*co*-loaded (PAH-D-CO_2/PSS)*10-(DAR/PSS)*4 films were cross-linked under UV irradiation to convert the ionic bonds between DAR and PSS into covalent sulfonate esters.[20] As judged from UV−vis absorption spectra, although the loading of MO and R6G in (PAH-D-CO_2/PSS)*10-(DAR/PSS)*4 films proceeds slowly, the amounts of MO and R6G loaded in the (PAH-D-CO_2/PSS)*10 films with barrier layers are almost the same as those without barrier layers. As shown in Figure 5b, the simultaneous release of MO and R6G from the cross-linked (DAR/PSS)*4-capped (PAH-D-CO_2/PSS)*10 films in 0.9% normal saline is largely prolonged. All the loaded MO molecules in the (PAH-D-CO_2/PSS)*10 films capped with cross-linked (DAR/PSS)*4 films can be released. About 80% of the loaded R6G molecules are released after a 4-day immersion in 0.9% normal saline. The complete release of R6G is found difficult and takes longer time. It is reasonable to accept that the incorporation of barrier layers within the PAH-D-CO_2/PSS films can also be used to regulate and prolong the release kinetics of the loaded organic molecules.[3] Therefore, we believe that the rapid release of guest materials from polyampholyte microgel films can be overcome by the rational design of barrier layers while the large loading capacity of the polyampholyte microgel films can be fully utilized.

Stability of PAH-D-CO_2/PSS Multilayer Films. To testify the stability of PAH-D-CO_2/PSS multilayer films, a (PAH-D-CO_2/PSS)*10 film was first loaded with MO. After release of MO, the (PAH-D-CO_2/PSS)*10 film was used to load and release of R6G. These processes of loading and release of MO and R6G were repeated. As shown in Figure 6, the absorption peaks of MO at 433 nm and R6G at 544 nm fluctuated regularly with the successive loading and release of MO and R6G molecules. This result confirms the following: (i) No dissolution or peeling off of the PAH-D-CO_2/PSS films occurred during the successive loading and release process of MO and R6G molecules. (ii) The carbamate groups in PAH-D-CO_2/PSS films are chemical stable for long-term usage.

Structural Characterization of PAH-D-CO_2/PSS Multilayer Films. The thicknesses of a (PAH-D-CO_2/PSS)*10 film before and after loading of MO and R6G molecules were determined from their corresponding cross-sectional SEM images. As shown in Figure 7a, the (PAH-D-CO_2/PSS)*10 film before dye loading has a constant thickness of 112.8 ± 18.5 nm, corresponding to a thickness of 11.3 nm for one bilayer of PAH-D-CO_2/PSS.

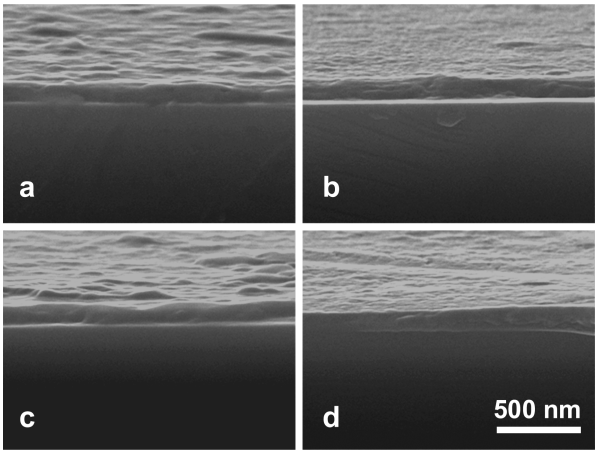

Figure 7. Cross-sectional SEM images of (PAH-D-CO_2/PSS)*10 films: (a) as-prepared; (b) after saturation loading of MO molecules; (c) after saturation loading of R6G molecules; (d) after coloading of MO and R6G molecules.

After independent loading of MO (Figure 7b) and R6G (Figure 7c), their thicknesses increased to be 145.2 ± 18.5 and 149.6 ± 8.6, which is ~1.29 and ~1.33 times thicker than its original thickness, respectively. Considering that the thicknesses of the PAH-D-CO_2/PSS films after independent loading of MO and R6G are 14.5 and 15.0 nm per bilayer, the densities of loaded MO and R6G in the films are as large as 0.16 and 0.15 g/cm^3, respectively. After coloading of MO and R6G (Figure 7d), the thickness of (PAH-D-CO_2/PSS)*10 film increased to be 153.6 ± 22.0 nm, which is ~1.36 times thicker than its original thickness. The high loading capacity of the PAH-D-CO_2/PSS microgel films can be understood as follows:[8] On the one hand, there are many amine and carbamate groups in the PAH-D-CO_2 layers, which provide abundant binding sites for MO and R6G molecules; on the other hand, slightly cross-linked PAH-D-CO_2 microgel layers make the multilayer film easily swollen in aqueous solution during the adsorption of MO and R6G molecules, which facilitate the penetration of dyes into the film and guarantee the availability of amine and carbamate groups for binding of dyes. In addition, the loading capacity of PAH-D-CO_2/PSS films for MO molecules is lower than that of PAH-D/PSS films because parts of amine groups in PAH-D microgels are converted into carbamate groups which reduced the number of binding sites for MO in PAH-D-CO_2/PSS films.

Conclusions

In this study, we have demonstrated a facile LbL assembly method to fabricate multilayer films capable of coloading oppositely charged dyes for their simultaneous release. The strategy of using PAH-D-CO_2 microgels as building blocks for LbL film fabrication lies in the following: (i) The polyampholyte PAH-D-CO_2 microgels contain an abundance of amine and carbamate groups, which can bind anionic and cationic dyes based on electrostatic interaction as a driving force. (ii) The cross-linked network of PAH-D-CO_2 microgels can swell in aqueous solution, which facilitates the penetration of dyes and guarantees their high loading amount. (iii) The PAH-D-CO_2 microgels are easily synthesized by bubbling CO_2 into aqueous solution of PAH-D microgels. Meanwhile, the LbL assembled multilayer films of PAH-D-CO_2/PSS with convenient preparation process can be, in principle, deposited on surfaces with complicated morphologies. The loading capacity of the PAH-D-CO_2/PSS films can be

conveniently adjusted by tailoring the assembly parameters for film deposition. Particularly, capping the PAH-D-CO_2/PSS films with photo-cross-linkable barrier layers can slow down the release kinetics of the polyampholyte microgel films. The above-mentioned advantages which originate from the LbL assembly method and the building blocks of polyampholyte PAH-D-CO_2 microgels are believed to make the LbL assembled PAH-D-CO_2/PSS multilayer films widely useful in the area of controlled release. We believe that LbL assembled polyampholyte microgel films, which are capable of coloading of large amounts of oppositely charged species, can be designed for the purpose of coloading and simultaneous release of oppositely charged drugs.

Acknowledgment. This work is supported by the National Natural Science Foundation of China (NSFC Grant No. 20974037), the National Basic Research Program (2007CB808000), and the Jilin Provincial Science and Technology Bureau of Jilin Province (20070104).

Supporting Information Available: SEM images, hydrodynamic diameter distribution curves and FTIR spectra of PAH-D and PAH-D-CO_2 microgels, UV−vis absorption spectrum of PAH-D-CO_2 cast film after loading of R6G. This material is available free of charge via the Internet at http://pubs.acs.org.